



Published in final edited form as:

J Immunol. 2008 September 15; 181(6): 4397–4405.

Evidence for an association between TSH and IGF-1 receptors:

A tale of two antigens implicated in Graves' disease¹

Shanli Tsui^{*}, Vibha Naik^{*}, Neil Hoa[¶], Catherine J. Hwang^{*,‡}, Nikoo F. Afifyan^{*}, Amiya Sinha Hikim[†], Andrew G. Gianoukakis^{*,†,§}, Raymond S. Douglas^{*,‡,§}, and Terry J. Smith^{*,†,‡,§,¶}

^{*}Division of Molecular Medicine, Department of Medicine, Harbor-UCLA Medical Center, Torrance, CA 90502

[†]Division of Endocrinology, Department of Medicine, Harbor-UCLA Medical Center, Torrance, CA 90502

[‡]Jules Stein Eye Institute, Los Angeles, CA 90095

[§]The David Geffen School of Medicine at UCLA, Los Angeles, CA 90095

[¶]Veterans Administration Medical Center, Long Beach, CA 90822

Abstract

TSH receptor (TSHR) plays a central role in regulating thyroid function and is targeted by IgGs in Graves' disease (GD-IgG). Whether TSHR is involved in the pathogenesis of thyroid associated ophthalmopathy, the orbital manifestation of GD, remains uncertain. TSHR signaling overlaps with that of insulin-like growth factor 1 receptor (IGF-1R). GD-IgG can activate fibroblasts derived from donors with GD to synthesize T cell chemoattractants and hyaluronan, actions mediated through IGF-1R. Here we compare levels of IGF-1R and TSHR on the surfaces of TAO and control orbital fibroblasts and thyrocytes and explore the physical and functional relationship between the two receptors. TSHR levels are 11-fold higher on thyrocytes than on TAO or control fibroblasts. In contrast, IGF-1R levels are 3-fold higher on TAO vs control fibroblasts. In pull-down studies using fibroblasts, thyrocytes and thyroid tissue, Abs directed specifically against either IGF-1R β or TSHR bring both proteins out of solution. Moreover, IGF-1R β and TSHR co-localize to the perinuclear and cytoplasmic compartments in fibroblasts and thyrocytes by confocal microscopy. Examination of orbital tissue from patients with TAO reveals similar co-localization to cell membranes. Treatment of primary thyrocytes with rhTSH results in rapid Erk phosphorylation which can be blocked by an IGF-1R-blocking monoclonal antibody. Our findings suggest that IGF-1R might mediate some TSH-provoked signaling. Further, they indicate that TSHR levels on orbital fibroblasts are considerably lower than those on thyrocytes and that this receptor associates with IGF-1R *in situ* and together may comprise a functional complex in thyroid and orbital tissue.

Keywords

thyroid; fibroblast; Graves' disease; autoimmune; thyrotropin receptor; insulin-like growth factor receptor

¹This work was supported in part by grants EY011708, EY008976, EY016339, DK063121, RR017304 and HD39293 from the National Institutes of Health, by a Merit Review award from the Research Service of the Department of Veterans Affairs, and by the Bell Charitable Trust.

Address all correspondence to: Terry J. Smith, M.D., Division of Molecular Medicine, Building C-2, Harbor-UCLA Medical Center, 1124 West Carson St., Torrance, CA 90502 tjsmith@ucla.edu.

Introduction

Insulin-like growth factor 1 receptor (IGF-1R) represents a ubiquitously expressed heterotetrameric protein involved in the regulation of proliferation and metabolic function of many cell types (1,2). It is a tyrosine kinase receptor comprising two subunits. IGF-1R α contains a ligand binding domain while IGF-1R β is involved in signaling and contains tyrosine phosphorylation sites. IGF-1R is involved in signaling that leads to a diverse set of cellular responses, including those involved in the modulation of apoptosis, through the PI3 kinase/AKT/FRAP/mTOR/p70^{S6k} pathway (3). Its pathway plays diverse roles in thymic development and immune function through IGF-1R display and activation in B and T cells (4-6). In contrast to IGF-1R, the thyrotropin receptor (TSHR), while expressed by several other cell and tissue types at low levels (7,8), appears to dominate regulatory function only in thyroid epithelium (9). TSHR mediates the influence TSH exerts on specialized thyroidal function. Most of the downstream signaling provoked by TSHR occupancy occurs as a consequence of its interactions with G proteins and the activation of adenylate cyclase (9). TSHR possesses an expansive ligand binding ectodomain linked by disulfide bonds to the membrane-anchoring domain. Like other members of the G-protein coupled receptor family, TSHR can dimerize. While the functional consequence of associating with other receptors is not yet understood, complex formation might modulate TSH action and receptor activation.

Graves' disease (GD) is an autoimmune disease where pathogenic Abs (GD-IgG) activate TSHR leading to over-production of thyroid hormone and accelerated metabolism of many tissues (10). Another component of GD is an orbital process, termed thyroid-associated ophthalmopathy (TAO), where connective tissue and fat expand, in part from accumulating hyaluronan, and become infiltrated with T and B cells, and extensively remodeled (11). It has been suggested that TSHR might have some pathogenic role in the development of TAO (12). Indeed, a positive correlation has been found between anti-TSHR Abs and the activity of TAO (13). TSHR mRNA has been detected, usually by PCR, in orbital tissues from patients with TAO (7) as well as in orbital fibroblasts derived from these patients, albeit at low levels (14). But no convincing link has been identified thus far establishing a role of TSHR or the Abs against it in the pathogenesis of TAO. On the other hand, GD-IgG can induce orbital fibroblasts from patients with TAO to produce hyaluronan (15) cells in which it instigates T cell chemoattractant expression, including up-regulating the synthesis of IL-16 and RANTES (16). These effects are absent in fibroblasts from normal controls and are mediated through IGF-1R (17). Thus, the trafficking of lymphocytes to the orbit and the disordered accumulation of hyaluronan in TAO might be explained, at least in part, by interactions between GD-IgG and IGF-1R.

Potential functional relationships between the TSHR and IGF-1R pathways were first suggested from studies reported nearly 20 years ago. Utilizing the clonal rat thyroid follicular cell line, FRTL-5, Ingbar and his colleagues demonstrated that IGF-1 could enhance TSH actions *in vitro* (18-21). No evidence to our knowledge has been advanced previously suggesting a physical association between TSHR and IGF-1R. Such a link could potentially help explain the permissive effects of IGF-1 on TSH-dependent thyroid function and growth. Here, we compare for the first time cell-surface TSHR and IGF-1R protein levels on orbital fibroblasts from control donors and patients with TAO with those on primary human thyroid epithelial cells (thyrocytes). TSHR levels are similar on control and TAO-derived orbital fibroblasts but are dramatically lower than those found on thyrocytes. TSHR levels increase substantially when fibroblasts are differentiated *in vitro* into fat cells. In contrast, IGF-1R levels are considerably higher *a priori* on the TAO orbital fibroblasts than those from control donors. These differences are mirrored by immunostaining orbital tissue *in situ*. Immunoprecipitation of either IGF-1R β or TSHR from human orbital fibroblasts, thyrocytes, or thyroid tissue results in an insoluble complex containing both receptors. They co-localize as revealed by confocal

microscopy in orbital fibroblasts and thyrocytes. The rapid activation of ERK in primary human thyrocytes by rhTSH could be attenuated with IGF-1R-blocking monoclonal antibodies, suggesting that TSHR and IGF-1R might form a functional complex. These unexpected results might explain the molecular basis for GD-IgG triggering multiple manifestations of GD.

Materials and Methods

Anti-human IGF-1R α (SC-712), IGF-1R β (sc-713), phosphorylated Erk (sc16982) and those directed against human TSHR (MCA1281 and sc-13936) were purchased from Santa Cruz (Santa Cruz, CA) or Serotec (Raleigh, NC). Secondary antibodies were from Vector Laboratories (Burlingame, CA). rhTSH was from Sigma (St. Louis, MO) and rIGF-1 was purchased from R&D Systems (Minneapolis, MN). The monoclonal antibody, 1H7 was supplied by Pharmingen (San Diego, CA). Specific siRNA for IGF-1R was purchased from Qiagen (Valencia, CA).

Cell culture

Human orbital fibroblasts were harvested and propagated as described previously (22). They were obtained from patients undergoing orbital surgery for severe TAO or for some medical condition not involving orbital inflammation. Explants were allowed to attach to plastic culture dishes and were covered with Eagle's minimal essential medium or Dulbecco's medium supplemented with 10% FBS, glutamine, and antibiotics. They were maintained in a 5% CO₂, humidified environment at 37°C. Explants were removed after fibroblasts encircled them and passaged by gentle treatment with trypsin/EDTA. They were utilized between the 2nd and 12th passage and were stored in liquid N₂. They were determined not to express Factor VIII, cytokeratin, or smooth muscle-specific actin (23). Human primary thyrocytes were obtained from surgical waste as described (24). They were covered with RPMI medium, passaged with trypsin treatment and used between the second and 6th passage. These activities were approved by the Institutional Review Board of the Harbor-UCLA Medical Center. Donors were euthyroid at the time of participation in these studies. Control donors had no history of autoimmune disease and no biochemical or physical evidence of thyroid disease.

Immunoprecipitation and Western blot analysis

Confluent monolayers were washed in PBS and lysed in a buffer containing 50 mM Hepes, pH 7.5, 150 mM NaCl, 1.5 mM MgCl₂, 1 mM EDTA, 10% glycerol, 0.5 % Triton X 100, 100 mM NaF, 1 mM Na vanadate and 10 mM Na pyrophosphate. Proteins were solubilized and centrifuged at 13,000 x g for 15 min at 4°C. The supernatant was collected, an aliquot taken for protein determination by the Bio-Rad method, and 400 μ g protein was subjected to immunoprecipitation with anti-human IGF-1R α , IGF-1R β or anti-human TSHR polyclonal antibodies (1 μ g) at 4°C with gentle rotation for 16 h. Protein A conjugated CL-4B Sepharose beads (Sigma) were added to the complex and the mixture mixed for another 2 h. Beads were washed 3 times in a buffer containing 10 mM Hepes, pH 7.5, 50 mM NaCl, 10% glycerol, 0.1 % Triton X-100, 1 mM sodium vanadate and 1 mM PMSF. These were then suspended in 2 X sample buffer and boiled for 5 min before separation by 7% SDS-PAGE. Separated proteins were transferred to PVDF Immobilon membrane (Millipore) and probed with primary antibody against IGF-1R α (1:1000), IGF-1R β (1:1000) or TSHR (1:800). Membranes were washed and incubated with HRP-conjugated anti-rabbit secondary antibody. Blots were developed using the Super Signal Extended Duration Substrate system (Pierce). Studies involving the phosphorylation of Erk 1/2 involved treating the thyrocytes with the test agents as indicated in the legend to Fig. 6. To knock down IGF-1R expression siRNA was incubated with the cultures for 96 h following the instructions of the supplier.

Confocal microscopy

Immunofluorescence staining and confocal microscopy were performed essentially as described previously (25). Briefly, cells adherent to glass cover slips were fixed in 2% paraformaldehyde in PBS for 30 min and permeated with 0.2% Triton-X 100 for 30 min. Following rinses in PBS, they were incubated with anti-IGF-1R α , anti-IGF-1R β or anti-TSHR antibodies alone or in combination at a dilution of 1:100 in PBS containing 5% goat serum for 2 hr. followed by incubation FITC- or Texas red-conjugated secondary antibody from Vector (Burlingame, CA) for 45 min. Coverslips were rinsed and mounted on glass slides with Vectashield mounting medium. Images were acquired and analyzed using a Nikon Eclipse 800 microscope interfaced with a Nikon PCM 2000 two-laser confocal system (Melville, NY).

Flow cytometry

Techniques utilized in these studies have been published previously (26). Briefly, 1×10^6 cells were placed in 12×75 mm polypropylene tubes and fluorochrome-conjugated monoclonal antibodies were added ($1 \mu\text{g}/10^6$ cells). These were then incubated in the dark for 20 min at room temperature. FACSlyse solution (2 ml) was added for 10 min at room temperature to disrupt RBCs. Cells were washed twice with SB, re-suspended in Cytfix (BD Biosciences, San Jose, CA) and kept in the dark at 4°C until cytometric analysis (within 24 h). Analysis was performed on a FACS Calibur flow cytometer (BD Biosciences). Mean fluorescent intensity (M.F.I.) was calculated as a ratio of mean fluorescence sample / isotype fluorescence. To quantify binding sites represented by fluorescence signals, $50 \mu\text{l}$ of Quantum Simply Cellular Microbeads (Sigma) were incubated with $10 \mu\text{l}$ IGF-IR, $10 \mu\text{l}$ TSH-R or isotype antibody for 30 min at room temperature. The bead standards consisted of four populations of simply cellular microbeads coated with goat anti-mouse antibody which bind a different number of mouse IgG monoclonal antibody molecules (4,063; 14,354; 54,401; 203,303 molecule binding capacity) and a blank population. The beads were then washed three times with staining buffer. Flow cytometric analysis was performed using the same settings as for cell analysis. A histogram of red fluorescence (FL2) was produced for the beads and the mean fluorescence channel number for each peak was taken. A best fit curve was drawn to relate linear channel number to logarithmic binding capacity (molecules) from which values for the IGF-IR samples and isotype control samples could be read. These values were subtracted in order to account for autofluorescence and non-specific binding (QuickCal, QSC calibration software). To calibrate the fluorescence scale of the flow cytometer, we determined the antibody binding capacity (ABC) which represents the number of Ab molecules bound on each cell or micro-bead. ABCs were calculated by subtracting control staining from that generated with anti-IGF-1R and anti-TSHR Abs.

Quantification of fibroblast number

Fibroblasts were cultured as described above. Cell counts were determined according to the manufacturer's protocol (CyQuant; Invitrogen, Carlsbad CA). Briefly, cells were cultured in 96 well plates and incubated for 24 hours to 7 days. At the desired time, plates were frozen at -70°C until analysis. Culture solution did not contain Phenol Red since the dye can interfere with CyQuant GR dye fluorescence. Plates were thawed at room temperature and $200 \mu\text{l}$ of CyQuant GR dye/cell lysis buffer was added to each well and incubated for 5 minutes with gentle mixing. Samples were protected from light and emissions were determined using a Wallac Victor 1420 fluorometer (Perkin Elmer) at 480 nm excitation and 520 nm emission wave-lengths. They were assayed in quadruplicate and compared to a standard curve.

Statistics—Data are expressed as the mean \pm SEM. Statistical significance was determined by Student's *t* test.

Results

IGF-1R is over-expressed by orbital fibroblasts from patients with TAO compared to control donors while TSHR levels are low in fibroblasts from both sets of donors

Three strains of orbital fibroblasts, each from a different donor were examined for IGF-1R and TSHR cell surface display by flow cytometry, as shown in Fig. 1. As the individual cytometric profiles demonstrate, IGF-1R levels are substantially higher in each cell strain as is indicated by the shift away from that of the isotype control. In contrast, TSHR levels in both GD- and control fibroblasts are vanishingly low and their profiles are very similar to those generated by the isotype control Abs. IGF-1R levels were then examined in a total of 9 different TAO strains compared with 5 control fibroblast strains (Fig. 2A). The mean fluorescence intensities (MFIs) were dramatically higher in those strains from TAO donors and the data from the two sources did not overlap (TAO, 3-fold, $p < 0.003$ vs control). Relative receptor densities, as reflected in the MFIs were substantially and significantly different as were results from the ABC analysis (Fig 2B, $p < 0.01$). In contrast, TSHR protein levels appear similar in TAO and control fibroblasts, although the disease-derived strains exhibit higher receptor densities than do 4/5 of the normal controls. TSHR levels in all 10 fibroblast strains examined were dramatically lower than those found in primary thyrocytes (11-fold difference, $p < 1 \times 10^{-6}$). In paired studies, orbital fibroblasts from patients with TAO display high levels of IGF-1R but fail to express detectable surface TSHR (Fig. 3A). In contrast, thyrocytes, in this case from a patient with GD express high levels of both receptors.

Differentiation of orbital fibroblasts from patients with TAO into adipocytes leads to increased surface TSHR levels as well as to accumulation of Oil Red O droplets (Fig. 3B and insets). While levels may fail in some studies to approximate those found on thyrocytes, they increase approximately 8-fold above undifferentiated fibroblasts. In contrast, control orbital fibroblasts incubated under identical conditions failed to differentiate or to display elevated TSHR levels. As in other models of adipocyte differentiation, IGF-1R levels fail to change (data not shown).

Relatively high IGF-1R levels on TAO fibroblasts result in proliferation when treated with IGF-1

As the data in Fig. 4 demonstrate, TAO orbital fibroblasts appear to proliferate more rapidly, even under control culture conditions, than do their counterparts from individuals without GD. Treatment of disease-derived fibroblasts with IGF-1 (10 nM or 50 nM) for 7 days resulted in concentration-dependent cell proliferation compared to that seen in control fibroblast cultures. In contrast, treatment of orbital fibroblasts from either donor-source with rhTSH (2 mU/ml) under identical conditions failed to alter fibroblast proliferation. This absence of an effect differs from the findings in cultured rat preadipocytes (27) where extremely high concentration of TSH (30 μ M) caused substantial proliferation.

Immunolocalization of IGF-1R α , IGF-1R β and TSHR in orbital fibroblasts, primary thyrocytes, and intact orbital tissue by confocal microscopy—TSHR was detected using a FITC conjugated secondary Ab against a rabbit polyclonal anti-TSHR Ab (green). Detection of IGF-1R β was accomplished with a Texas red-conjugated secondary Ab against a mouse monoclonal anti-IGF-1R β antibody (red). As shown in Fig. 5 (panels A-F), IGF-1R β was localized to the periphery of both orbital fibroblasts and thyrocytes as well as to the perinuclear area, a distribution that was identical to the staining pattern of TSHR. The yellow or orange staining seen in the merged images (panels C and F) results from co-localization of IGF-1R β and TSHR. Thyrocytes exhibit particularly heavy membrane TSHR staining that dominates the IGF-1R β signal, as is evident in the merged image where green color is retained in the cell periphery. Perinuclear localization of both receptors was confirmed by the characteristic yellow color evident over the nuclear area when the images are merged.

To verify the specificity of the respective signals, a second pair of Abs was tested. In this case, the primary anti-TSHR Ab utilized was monoclonal and that directed against IGF-1R β was polyclonal. As the images in panels G and H attest, staining with this second Ab pair was very similar to that seen with the first set of Abs with regard to localization of the receptors. The merged image found in panel I again demonstrates the co-localization of the two receptors.

IGF-1R α was detected using a Texas red conjugated secondary Ab against the mouse monoclonal anti-IGF-1R α Ab (red). As shown in Fig. 5 (panel J), intense TSHR staining could again be localized to the perinuclear areas of orbital fibroblasts. Weak to moderate immunostaining was also noted in the central region of the cells. In contrast, IGF-1R α was cytosolic and predominantly localized in the perinuclear and central regions of the cell but was absent from the nucleus (Fig. 5, panel K). TSHR was found to be co-localized with IGF-1R α , as is evidenced by double immunostaining of these proteins. The yellow staining seen in the merged panel (Fig. 5, panel L) resulted from co-localization of the green TSHR and red IGF-1R α .

IGF-1R staining in orbital fat from patients with TAO

We have also examined IGF-1R staining in orbital tissues *in situ* to determine whether the co-localization occurring in cultured cells was relevant to the intact human orbit. Tissue from patients with TAO exhibits specific staining for IGF-1R (Fig. 5N, red) that outlines the surfaces of fat cells and extends to fibroblasts. In contrast, staining for TSHR (Fig. 5M, green) in orbital tissue is relatively scant. As the image in Fig. 5O demonstrate, when the images of IGF-1R β and TSHR are merged, areas of orange appear, demonstrating co-localization peripherally to plasma membranes of the cells outlined. Thus the pattern of co-localization found in cultured orbital fibroblasts was also detected *in vivo*.

Immunoprecipitation of IGF-1R α , IGF-1R β and TSHR in orbital fibroblasts, primary thyrocytes and thyroid tissue

IGF-1R is expressed by many different cell types, including cultured human fibroblasts (28) and thyrocytes (29). As the Western blot in Fig. 6A demonstrates, both IGF-1R β and TSHR can be detected in these two cell-types as well as in thyroid tissue. We next determined whether each receptor could be detected in the immunoprecipitate resulting from treating cell and tissue lysates with Abs against IGF-1R and TSHR. When the homogenates were subjected to precipitation with Abs directed against IGF-1R β , TSHR as well as IGF-1R β were both detectable by western blot as was IGF-1R α (Fig. 6A). Similarly, when the samples were immunoprecipitated with anti-TSHR Ab, both receptors proved abundant in the precipitated complex. In contrast, IGF-1R β or TSHR could not be detected in the immunoprecipitate resulting from an irrelevant Ab, such as anti-IL-6R (designated “control” in the figure). When orbital fibroblast lysates were immunoprecipitated with anti-TSHR Ab, IGF-1R α was not detected while IGF-1R β was abundant in the insoluble material (Fig. 6B). These results strongly suggest that IGF-1R β and TSHR form a relatively tight complex. This complex was disrupted when cells were treated with specific siRNA to down-regulate IGF-1R expression (Fig. 6C). In contrast, IGF-1R α fails to co-precipitate with TSHR, suggesting that the co-localization of the two demonstrated by confocal microscopy (Fig. 5) results in a weaker association. On the other hand, IGF-1R α and IGF-1R β co-precipitate, as expected.

Activation by TSH of Erk in thyrocytes involves the IGF-1R

We next tested whether the association of TSHR and IGF-1R had functional consequences. Thyrocytes were treated with rhTSH (1 mU/ml) for 15 min. Monolayers were harvested and subjected to western blot analysis for phosphorylated Erk. As the immunoblot in Fig. 6D indicates, TSH rapidly activates Erk. When the IGF-1R-blocking mAb, 1H7 (30) (5 μ g/ml)

was added to the medium in addition to rhTSH, it could completely block the activation of Erk. These results directly implicate IGF-1R in the action of TSH on human thyrocytes.

Discussion

Uncertainty about the pathogenesis of TAO and its relationship to intra-thyroidal GD has led to the suggestion by some that TSHR might play a role in both disease processes. A substantial and sometimes conflicting body of evidence supports the concept that TSHR is expressed in the human orbit and may be elevated in active TAO (7,31-34). TSHR mRNA is expressed in cultured orbital fibroblasts and receptor levels are increased following adipogenic differentiation (14,35,36) when its Immunostaining becomes more intense (35). In contrast, TSHR mRNA levels fail to change in orbital fibroblasts from normal donors following differentiation, although Valyasevi et al (14) reported that receptor levels and TSH-dependent cAMP generation increased more in these control cells. Several studies have demonstrated increased intracellular cAMP levels in fibroblasts in response to TSH (14,35,36). But the levels achieved were modest and the concentrations of TSH used were extremely high, calling into question their biological significance. Thus it remains an open question whether the low TSHR levels found expressed by orbital fibroblasts are adequate for eliciting immunological reactivity or for initiating cell signaling relevant to TAO.

In this report, we demonstrate extremely low levels of surface TSHR protein on orbital fibroblasts compared to those seen on thyrocytes. No consistent differences in receptor levels were found in fibroblasts from patients with TAO and normal controls, although the former trended to a somewhat higher abundance. Once differentiated, TAO orbital adipocytes express considerably higher TSHR protein levels than do their undifferentiated precursors or their normal counterparts. Thus, it seems logical to postulate that any functional role for TSHR expressed by connective tissue in the pathogenesis of TAO probably requires prior cell differentiation. A number of laboratory groups have also reported TSHR expression in human connective/fatty tissues outside the orbit and by their derivative fibroblasts (8,37,38). Further, TSHR expression appears widespread in rodent fat (39) and TSHR mRNA levels in rat testicular fat approach those in thyroid (40). Therefore, any theoretical model attempting to explain the anatomic site-selective manifestations of GD on the basis of TSHR must be reconciled with the evidence for widespread receptor expression in fat (12). Another ubiquitously expressed protein, IGF-1R, has also been implicated in the development of TAO. GD-derived fibroblasts *a priori* display substantially higher levels of IGF-1R than do their normal counterparts. Using ABC analysis with flow cytometry, the density of IGF-1R is 3-fold above levels seen in controls (Fig. 2). IGF-1R levels in TAO-derived fibroblasts are associated with disease-associated cellular responses, such as the induction of IL-16 and RANTES (16,17), both of which may play roles in experimental models and in human autoimmune disease (41,42). It is possible that T cell trafficking to affected tissues in GD results from the expression of these or related chemoattractants.

Our current findings also suggest that TSHR and IGF-1R co-localize to the perinuclear, cytoplasmic, and plasma membrane compartments of human orbital fibroblasts and thyrocytes. A number of previous studies have raised the potential for functional interplay between heterotrimeric G proteins and IGF-1 signaling. For instance, Erk 1/2 activation provoked by IGF-1 is pertussis toxin sensitive and may require the participation of $G_{\beta\gamma}$ mediated signaling in RAT1 fibroblasts (43). This finding was confirmed with expression of a $G_{\beta\gamma}$ -binding peptide leading to the interruption of IGF-1R signaling provoking Erk 1/2 phosphorylation. Recently, El-Shewy *et al* suggested that IGF-1 might activate Erk 1/2 through G protein trans-activating sphingosine 1-phosphate receptors (44). On the other hand, IGF-1 might also enhance some but not all TSHR signaling, a strong possibility based on several earlier reports. For instance, Tramontano *et al* found that both IGF-1 and TSH could enhance FRTL-5 cell proliferation and

DNA synthesis in a concentration-dependent manner and that these actions were synergistic (18). In contrast, TSH-dependent cAMP generation appears not to be influenced by IGF-1 in FRTL-5 cells (18-21). More recently, Clement and colleagues demonstrated that the conditional over-expression of both IGF-1 and IGF-1R in the thyroid of double-transgenic mice results in increased thyroid gland weight and area of the follicular lumen *in vivo* (45). In addition, these animals exhibited decreased serum TSH and a slightly elevated thyroxine level, suggesting enhanced sensitivity to TSH (45). Thus, it would appear that IGF-1 and its receptor may enhance the impact of TSH on thyroid function and growth *in vivo*. Our finding that treatment of thyrocytes with TSH results in Erk 1/2 phosphorylation that can be attenuated with an IGF-1R α blocking Ab suggests that previously recognized signaling downstream from TSHR, including the activation of p66Shc (46), Jak/STAT (47), and SOCS-1 (48) might involve IGF-1R transactivation. Cass and Meinkoth reported that the ligated TSHR could activate p70^{S6k} pathway in thyrocytes (49). This pathway can be activated in FRTL-5 cells by TSH and TSHR-stimulating antibodies from patients with GD (50). The authors suggested an interaction between TSHR and PI₃ kinase as the basis for this signaling pattern. Saunier *et al* found that TSH could activate p42 Erk in primary human thyrocytes, that the effects were attenuated with TSHR-blocking antibodies and were mediated through a pertussis toxin-insensitive pathway (51). Vandeput and colleagues reported treatment with rhTSH and bTSH resulted in modest activation of Erk in human thyrocytes but not in those from dog (52). The authors ruled out involvement of Gq in this effect and could not attenuate the activation of Erk with TSH neutralizing antibodies, although that strategy blocked cAMP generation. They concluded that both rhTSH and bTSH were contaminated with an uncharacterized substance that initiated this pattern of signaling. Our findings not only confirm this TSH effect on Erk phosphorylation (Fig. 6D), but suggest that TSHR and IGF-1R β form an insoluble complex and that tyrosine phosphorylation sites on IGF-1R β might mediate some aspects of TSHR signaling. Thus, our findings suggest that a physical and functional association between TSHR and IGF-1R could mediate aspects of signaling traditionally attributed to each receptor alone.

Precedent for intracellular localization of both tyrosine kinase and G protein-coupled membrane receptors abounds. IGF-1R β can internalize following its ligation (53) and can localize to the cell nucleus (54). Moreover, epidermal growth factor receptor translocates to the nucleus and functions as a transcriptional factor (55). Little information currently exists regarding TSHR distribution in cell monolayers, such as those used in these studies. Baratti-Elbaz *et al* described recently the intracellular trafficking of TSHR and its recycling to the cell surface in cells over-expressing the protein (56). Epithelial cell polarity can be lost when tissue orientation becomes disrupted (57-59), thus offering a potential explanation for different distribution of TSHR in cell monolayers. TSHR density is usually greatest in the basolateral membrane in the thyrocytes comprising intact follicles as well as in transfected L cells (56, 60,61). Other G protein coupled receptors, including those for LH-RH, apelin, angiotensin and bradykinin, have been shown to localize to the cell nucleus (62,63). The high perinuclear concentrations of TSHR demonstrated in the current studies could represent similar compartmentalization. Thus, earlier findings coupled with those we now report strongly suggest additional biological roles for surface receptors occurring inside the cell, functioning either as individual proteins or as complexes.

Vanishingly little detail has been uncovered thus far concerning the precise nature of the immune responses in GD that underlie site-specific immune infiltration of thyroid and orbit. We recognize the importance to disease pathogenesis of Abs generated against TSHR (10) but have reported very recently that IgGs from these patients can also activate IGF-1R, an interaction that induces expression of T cell chemoattractants (16,17,64) and hyaluronan (15). Thus, IGF-1R may represent a second self-antigen, in addition to TSHR, relevant to the pathogenesis of GD. The physical association between them, as is implied by our current findings, may play some as yet undetermined role in Ab generation. One possibility concerns

potentially exaggerated exposure of auto-reactive T cells and B cells to increased numbers and diversity of antigens resulting from epitope spread. This process can enhance the amplitude of immune reactivity and promote antigen-specific tissue targeting by immunocompetent cells (65-67). Antigenic presentation and recognition of IGF-1R and TSHR through innate and cognate responses could broaden and intensify those responses. Thus, immunity associated with GD may prove analogous to that occurring in allied diseases such as Type 1 diabetes mellitus and SLE, where a stepwise generation of new auto-antigens results in multiple disease manifestations (68-70). Identifying neo-antigens relevant to GD and determining whether epitope spreading plays a role in their generation should put our current findings into a more complete context.

Acknowledgments

The authors wish to thank Ms. Debbie Hanaya for expert assistance in preparing this manuscript.

References

1. Adams TE, Epa VC, Garrett TPJ, Ward CW. Structure and function of the type I insulin-like growth factor receptor. *Cell Mol. Life Sci* 2000;57:1050–1093. [PubMed: 10961344]
2. De Meyts P, Whittaker J. Structural biology of insulin and IGF1 receptors: implications for drug design. *Nature Rev* 2002;1:769–783.
3. Dupont J, Fernandez AM, Glackin CA, Helman L, LeRoith D. Insulin-like growth factor 1 (IGF-1)-induced twist expression is involved in the anti-apoptotic effects of the IGF-1 receptor. *J. Biol. Chem* 2001;276:26699–26707. [PubMed: 11323435]
4. Binz K, Joller P, Froesch P, Binz H, Zapf J, Froesch ER. Repopulation of the atrophied thymus in diabetic rats by insulin-like growth factor I. *Proc. Natl. Acad. Sci. USA* 1990;87:3690–3694. [PubMed: 2187189]
5. Kooijman R, Scholtens LE, Rijkers GT, Zegers BJM. Differential expression of type I insulin-like growth factor receptors in different stages of human T cells. *Eur. J. Immunol* 1995;25:931–935. [PubMed: 7737296]
6. Landreth KS, Narayanan R, Dorshkind K. Insulin-like growth factor-I regulates pro-B cell differentiation. *Blood* 1992;80:1207–1212. [PubMed: 1515639]
7. Feliciello A, Porcellini A, Ciullo I, Bonavolonta G, Avvedimento EV, Fenzi G. Expression of thyrotropin-receptor mRNA in healthy and Graves' disease retro-orbital tissue. *Lancet* 1993;342:337–338. [PubMed: 8101586]
8. Agretti P, Chiovato L, De Marco G, Marcocci C, Mazzi B, Sellari-Franceschini S, Vitti P, Pinchera A, Tonacchera M. Real-time PCR provides evidence for thyrotropin receptor mRNA expression in orbital as well as in extraorbital tissues. *Eur. J. Endocrinol* 2002;147:733–739. [PubMed: 12457447]
9. Szkudlinski MW, Fremont V, Ronin C, Weintraub BD. Thyroid-stimulating hormone and thyroid-stimulating hormone receptor structure-function relationships. *Physiol. Rev* 2002;82:473–502. [PubMed: 11917095]
10. Davies, TF. Graves' disease. In: Braverman, LE.; Utiger, RD., editors. *Werner and Ingbar's The Thyroid*. Vol. 7th ed.. Lippincott-Raven Publishers; Philadelphia: 1996. p. 525-558.
11. Kazim M, Goldberg RA, Smith TJ. Insights into the pathogenesis of thyroid associated orbitopathy: Evolving rationale for therapy. *Arch. Ophthalmol* 2002;120:380–386. [PubMed: 11879144]
12. Paschke R, Vassart G, Ludgate M. Current evidence for and against the TSH receptor being the common antigen in Graves' disease and thyroid associated ophthalmopathy. *Clin. Endocrinol. (Oxf)* 1995;42:565–569. [PubMed: 7634495]
13. Gerding MN, van der Meer JW, Broenink M, Bakker O, Wiersinga WM, Prummel MF. Association of thyrotrophin receptor antibodies with the clinical features of Graves' ophthalmopathy. *Clin Endocrinol (Oxf)* 2000;52:267–271. [PubMed: 10718823]
14. Valyasevi RW, Erickson DZ, Harteneck DA, Dutton CM, Heufelder AE, Jyonouchi SC, Bahn RS. Differentiation of human orbital preadipocyte fibroblasts induces expression of functional thyrotropin receptor. *J. Clin. Endocrinol. Metab* 1999;84:2557–2562. [PubMed: 10404836]

15. Smith TJ, Hoa N. Immunoglobulins from patients with Graves' disease induce hyaluronan synthesis in their orbital fibroblasts through the self-antigen, IGF-1 receptor. *J. Clin. Endocrinol. Metabol* 2004;89:5076–5080.
16. Pritchard J, Horst N, Cruikshank W, Smith TJ. Igs from patients with Graves' disease induce the expression of T cell chemoattractants in their fibroblasts. *J. Immunol* 2002;168:942–950. [PubMed: 11777993]
17. Pritchard J, Horst N, Cruikshank WW, Smith TJ. Immunoglobulin activation of T cell chemoattractant expression in fibroblasts from patients with Graves' disease is mediated through the IGF-1 receptor pathway. *J. Immunol* 2003;170:6348–6354. [PubMed: 12794168]
18. Tramontano D, Cushing GW, Moses AC, Ingbar SH. Insulin-like growth factor-1 stimulates the growth of rat thyroid cells in culture and synergizes the stimulation of DNA synthesis induced by TSH and Graves'-IgG. *Endocrinology* 1986;119:940–942. [PubMed: 2874015]
19. Tramontano D, Moses AC, Picone R, Ingbar SH. Characterization and regulations of the receptor for insulin-like growth factor-1 in the FRTL-5 rat thyroid follicular cell line. *Endocrinology* 1987;120:785–790. [PubMed: 2948816]
20. Tramontano D, Moses AC, Veneziani BM, Ingbar SH. Adenosine 3'5'-monophosphate mediates both the mitogenic effect of thyrotropin and its ability to amplify the response to insulin-like growth factor-1 in FRTL-5 cells. *Endocrinology* 1988;122:127–132. [PubMed: 2446854]
21. Tramontano D, Moses AC, Ingbar SH. The role of adenosine 3'5'-monophosphate in the regulation of receptors for thyrotropin and insulin-like growth factor-1 in the FRTL-5 rat thyroid follicular cell. *Endocrinology* 1988;22:133–136. [PubMed: 2826109]
22. Smith TJ, Ahmed A, Hogg MG, Higgins PJ. Interferon gamma is an inducer of plasminogen activator inhibitor type-1 in human orbital fibroblasts. *Am. J. Physiol. Cell. Physiol* 1992;263:C24–C29.
23. Smith TJ, Sempowski GD, Wang H-S, Del Vecchio PJ, Lippe SD, Phipps RP. Evidence for cellular heterogeneity in primary cultures of human orbital fibroblasts. *J. Clin. Endocrinol. Metab* 1995;80:2620–2625. [PubMed: 7673404]
24. Gianoukakis AG, Cao HJ, Jennings TA, Smith TJ. Prostaglandin endoperoxide H synthase expression in cultured human thyroid epithelial cells. *Am. J. Physiol. Cell. Physiol* 2001;280:C701–C708. [PubMed: 11171589]
25. Sinha Hikim AP, Lue Y, Yamamoto CM, Vera Y, Rodriguez S, Yen PH, Soeng K, Wang C, Swerdloff RS. Key apoptotic pathways for heat-induced programmed germ cell death in the testis. *Endocrinology* 2003;144:3167–3175. [PubMed: 12810573]
26. Douglas RS, Gianoukakis AG, Kamat S, Smith TJ. Aberrant expression of the IGF-1 receptor by T cells from patients with Graves' disease may carry functional consequences for disease pathogenesis. *J. Immunol* 2007;178:3281–3287. [PubMed: 17312178]
27. Haraguchi K, Shimura H, Kawaguchi A, Ikeda M, Endo T, Onaya T. Effects of thyrotropin on the proliferation and differentiation of cultured rat preadipocytes. *Thyroid* 1999;9:613–619. [PubMed: 10411125]
28. Rosenfeld RG, Dollar LA. Characterization of the somatomedin-C/insulin-like growth factor I (SM-C/IGF-I) receptor on cultured human fibroblasts monolayers: regulation of receptor concentrations by SM-C/IGF-I and insulin. *J. Clin. Endocrinol. Metab* 1982;55:434–440. [PubMed: 6284779]
29. Maiorano E, Perlino E, Triggiani VV, Nacchiero M, Giove E, Ciampolillo A. Insulin-like growth factor receptor in thyroid tissues of patients with Graves' disease. *Int. J. Mol. Med* 1998;2:483–486. [PubMed: 9857239]
30. Li SL, Kato J, Paz IB, Kasuya J, Fujita-Yamaguchi Y. Two new monoclonal antibodies against the alpha subunit of the human insulin-like growth factor-1 receptor. *Biochem. Biophys. Res. Commun* 1993;196:92–98. [PubMed: 8216340]
31. Davies TF, Teng CS, McLachlan SM, Smith BR, Hall R. Thyrotropin receptors in adipose tissue, retro-orbital tissue and lymphocytes. *Mol. Cell. Endocrinol* 1978;9:303–310. [PubMed: 203502]
32. Wakelkamp IM, Bakker O, Baldeschi L, Wiersinga WM, Prummel MF. TSH-R expression and cytokine profile in orbital tissue of active vs. inactive Graves' ophthalmopathy patients. *Clin. Endocrinol. (Oxf)* 2003;58:280–287. [PubMed: 12608932]

33. Starkey KJ, Janezic A, Jones G, Jordan N, Baker G, Ludgate M. Adipose thyrotrophin receptor expression is elevated in Graves' and thyroid eye diseases ex vivo and indicates adipogenesis in progress in vivo. *J. Mol. Endocrinol* 2003;30:369–380. [PubMed: 12790806]
34. Wu SL, Yang CS, Wang HJ, Liao CL, Chang TJ, Chang TC. Demonstration of thyrotrophin receptor mRNA in orbital fat and eye muscle tissues from patients with Graves' ophthalmopathy by in situ hybridization. *J. Endocrinol. Invest* 1999;22:289–295. [PubMed: 10342363]
35. Agretti P, De Marco G, De Servi M, Marcocci C, Vitti P, Pinchera A, Tonacchera M. Evidence for protein and mRNA TSHr expression in fibroblasts from patients with thyroid-associated ophthalmopathy (TAO) after adipocytic differentiation. *Eur. J. Endocrinol* 2005;152:777–784. [PubMed: 15879364]
36. Crisp M, Starkey KJ, Lane C, Ham J, Ludgate M. Adipogenesis in thyroid eye disease. *Invest. Ophthalmol. Vis. Sci* 2000;41:3249–3255. [PubMed: 11006210]
37. Crisp MS, Lane C, Halliwell M, Wynford-Thomas D, Ludgate M. Thyrotrophin receptor transcripts in human adipose tissue. *J. Clin. Endocrinol. Metab* 1997;82:2003–2005. [PubMed: 9177421]
38. Bell A, Gagnon A, Grunder L, Parikh SJ, Smith TJ, Sorisky A. Functional TSH receptor in human abdominal preadipocytes and orbital fibroblasts. *Am. J. Physiol. Cell. Physiol* 2000;279:C335–C340. [PubMed: 10912999]
39. Endo T, Ohno M, Kotani S, Gunji K, Onaya T. Thyrotrophin receptor in non-thyroid tissues. *Biochem. Biophys. Res. Commun* 1993;190:774–779. [PubMed: 8439328]
40. Endo T, Ohta K, Haraguchi K, Onaya T. Cloning and functional expression of a thyrotrophin receptor cDNA from rat fat cells. *J. Biol. Chem* 1995;270:10833–10837. [PubMed: 7738021]
41. Franz JK, Kolb SA, Hummel KM, Lahrtz F, Neidhart M, Aicher WK, Pap T, Gay RE, Fontana A, Gay S. Interleukin-16, produced by synovial fibroblasts, mediates chemoattraction for CD4+ T lymphocytes in rheumatoid arthritis. *Eur. J. Immunol* 1998;28:2661–2671. [PubMed: 9754554]
42. Robinson E, Keystone EC, Schall TJ, Gillett N, Fish EN. Chemokine expression in rheumatoid arthritis (RA): evidence of RANTES and macrophage inflammatory protein (MIP)-1 β production by synovial T cells. *Clin. Exp. Immunol* 1995;101:398–407. [PubMed: 7545093]
43. Luttrell LM, van Biesen T, Hawes BE, Koch WJ, Touhara K, Lefkowitz RJ. G $\beta\gamma$ subunits mediate mitogen-activated protein kinase activation by the tyrosine kinase insulin-like growth factor 1 receptor. *J. Biol. Chem* 1995;270:16495–16498. [PubMed: 7622449]
44. El-Shewy HM, Johnson KR, Lee MH, Jaffa AA, Obeid LM, Luttrell LM. Insulin-like growth factors mediate heterotrimeric G protein-dependent ERK1/2 activation by transactivating sphingosine 1-phosphate receptors. *J. Biol. Chem* 2006;281:31399–31407. [PubMed: 16926156]
45. Clement S, Refetoff S, Robaye B, Dumont JE, Schurmans S. Low TSH requirement and goiter in transgenic mice overexpressing IGF-1 and IGF-1 receptor in the thyroid gland. *Endocrinology* 2001;142:5131–5139. [PubMed: 11713206]
46. Park YJ, Kim TY, Lee SH, Kim H, Kim SW, Shong M, Yoon YK, Cho BY, Park DJ. p66Shc expression in proliferating thyroid cells is regulated by thyrotrophin receptor signaling. *Endocrinology* 2005;146:2473–2480. [PubMed: 15705774]
47. Park ES, Kim H, Suh JM, Park SJ, You SH, Chung HK, Lee KW, Kwon OY, Cho BY, Kim YK, Ro HK, Chung J, Shong M. Involvement of JAK/STAT (Janus kinase/signal transducer and activator of transcription) in the thyrotrophin signaling pathway. *Mol. Endocrinol* 2000;14:662–670. [PubMed: 10809230]
48. Park ES, Kim H, Suh JM, Park SJ, Kwon OY, Kim YK, Ro HK, Cho BY, Chung J, Shong M. Thyrotrophin induces SOCS-1 (suppressor of cytokine signaling-1) and SOCS-3 in FRTL-5 thyroid cells. *Mol. Endocrinol* 2000;14:440–448. [PubMed: 10707961]
49. Cass LA, Meinkoth JL. Differential effects of cyclic adenosine 3',5'-monophosphate on p70 ribosomal S6 kinase. *Endocrinology* 1998;139:1991–1998. [PubMed: 9528986]
50. Suh JM, Song JH, Kim DW, Kim H, Chung HK, Hwang JH, Kim JM, Hwang ES, Chung J, Han J-H, Cho BY, Ro HK, Shong M. Regulation of the phosphatidylinositol 3-kinase, Akt/protein kinase B, FRAP/mammalian target of rapamycin, and ribosomal S6 kinase 1 signaling pathways by thyroid-stimulating hormone (TSH) and stimulating type TSH receptor antibodies in the thyroid gland. *J. Biol. Chem* 2003;278:21960–21971. [PubMed: 12668683]

51. Saunier B, Tournier C, Jacquemin C, Pierre M. Stimulation of mitogen-activated protein kinase by thyrotropin in primary cultured human thyroid follicles. *J. Biol. Chem* 1995;270:3693–3697. [PubMed: 7876108]
52. Vandeput F, Perpete S, Coulonval K, Lamy F, Dumont JE. Role of the different mitogen-activated protein kinase subfamilies in the stimulation of dog and human thyroid epithelial cell proliferation by cyclic adenosine 5'-monophosphate and growth factors. *Endocrinology* 2003;144:1341–1349. [PubMed: 12639917]
53. Vecchione A, Marchese A, Henry P, Rotin D, Morrione A. The Grb10/Nedd4 complex regulates ligand-induced ubiquitination and stability of the insulin-like-growth factor I receptor. *Mol. Cell. Biol* 2003;23:3363–3372. [PubMed: 12697834]
54. Chen C-W, Roy D. Up-regulation of nuclear IGF-I receptor by short term exposure of stilbene estrogen, diethylstilbestrol. *Mol. Cell. Endocrinol* 1996;118:1–8. [PubMed: 8735585]
55. Lin S-Y, Makino K, Xia W, Martin A, Wen Y, Yin Kwong K, Bourguignon L, Hung MC. Nuclear localization of EGF receptor and its potential new role as a transcription factor. *Nature Cell. Biol* 2001;3:802–808. [PubMed: 11533659]
56. Baratti-Elbaz C, Ghinea N, Lahuna O, Loosfelt H, Pichon C, Milgrom E. Internalization and recycling pathways of the thyrotropin receptor. *Mol. Endocrinol* 1999;13:1751–1765. [PubMed: 10517676]
57. Feracci H, Bernadac A, Hovsepian S, Fayet G, Maroux S. Aminopeptidase N is a marker for the apical pole of porcine thyroid epithelial cells in vivo and in culture. *Cell Tissue Res* 1981;221:137–146. [PubMed: 6119156]
58. Mauchamp J, Chambard M, Verrier B, Gabrion J, Chabaud O, Gerard C, Penel C, Pialat B, Anfosso F. Epithelial cell polarization in culture: orientation of cell polarity and expression of specific functions, studied with cultured thyroid cells. *J. Cell. Sci. Suppl* 1987;8:345–358. [PubMed: 3332666]
59. Fayet G, Hovsepian S. In vitro conversion of porcine thyroid cells growing in monolayer into functional follicular cells. *Biochimie* 1980;62:27–32. [PubMed: 7362840]
60. Beau I, Groyer-Picard M-T, Desroches A, Condamine E, Leprince J, Tome J-P, Dessen P, Vaudry H, Misrahi M. The basolateral sorting signals of the thyrotropin and luteinizing hormone receptors: an unusual family of signals sharing an unusual distal intracellular localization, but unrelated in their structures. *Mol. Endocrinol* 2004;18:733–746. [PubMed: 14694083]
61. Beau I, Misrahi M, Gross B, Vannier B, Loosfelt H, Vu Hai MT, Pichon C, Milgrom E. Basolateral localization and transcytosis of gonadotropin and thyrotropin receptors expressed in Madin-Darby canine kidney cells. *J. Biol. Chem* 1997;272:5241–5248. [PubMed: 9030595]
62. Halmos G, Schally AV. Changes in subcellular distribution of pituitary receptors for luteinizing hormone-releasing hormone (LH-RH) after treatment with the LH-RH antagonist cetrorelix. *Proc. Natl. Acad. Sci. USA* 2002;99:961–965. [PubMed: 11805337]
63. Lee DK, Lanca AJ, Cheng R, Nguyen T, Ji XD, Gobeil F Jr, Chemtob S, George SR, O'Dowd BF. Agonists-independent nuclear localization of the apelin, angiotensin AT₁, and bradykinin B₂ receptors. *J. Biol. Chem* 2004;279:7901–7908. [PubMed: 14645236]
64. Gianoukakis AG, Douglas RS, King CS, Cruikshank WW, Smith TJ. IgG from patients with Graves' disease induces IL-16 and RANTES expression in cultured human thyrocytes: A putative mechanism for T cell infiltration of the thyroid in autoimmune disease. *Endocrinology* 2006;147:1941–1949. [PubMed: 16410300]
65. Doyle HA, Mamula MJ. Posttranslational modifications of self-antigens. *Ann. N.Y. Acad. Sci* 2005;1050:1–9. [PubMed: 16014515]
66. Kent SC, Chen Y, Bregoli L, Clemmings SM, Kenyon NS, Ricordi C, Hering BJ, Hafler DA. Expanded T cells from pancreatic lymph nodes of type 1 diabetic subjects recognize an insulin epitope. *Nature* 2005;435:224–228. [PubMed: 15889096]
67. Nakayama M, Abiru N, Moriyama H, Babaya N, Liu E, Miao D, Yu L, Wegmann DR, Hutton JC, Elliott JF, Eisenbarth GS. Prime role for an insulin epitope in the development of type 1 diabetes in NOD mice. *Nature* 2005;435:220–223. [PubMed: 15889095]
68. Bonifacio E, Scirpoli M, Kredel K, Fuchtenbusch M, Ziegler AG. Early autoantibody responses in prediabetes are IgG1 dominated and suggest antigen-specific regulation. *J. Immunol* 1999;163:525–532. [PubMed: 10384157]

69. Yu L, Rewers M, Gianani R, Kawasaki E, Zhang Y, Verge C, Chase P, Klingensmith G, Erlich H, Norris J, Eisenbarth GS. Antiislet autoantibodies usually develop sequentially rather than simultaneously. *J. Clin. Endocrinol. Metab* 1996;81:4264–4267. [PubMed: 8954025]
70. Skyler JS, Krischer JP, Wolfsdorf J, Cowie C, Palmer JP, Greenbaum C, Cuthbertson D, Rafkin-Mervis LE, Chase HP, Leschek E. Effects of oral insulin in relatives of patients with type 1 diabetes: The Diabetes Prevention Trial—Type 1. *Diabetes Care* 2005;28:1068–1076. [PubMed: 15855569]

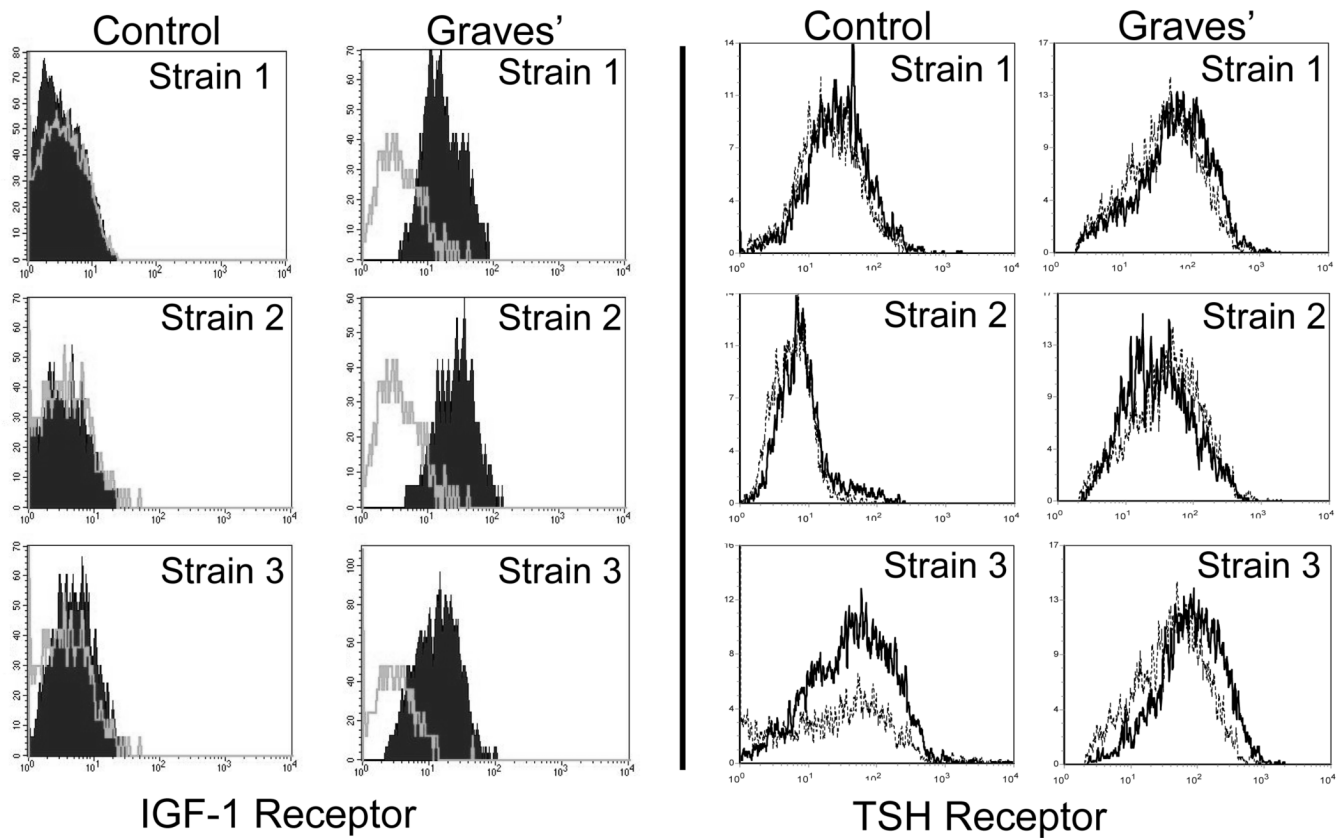


Figure 1.

Orbital fibroblasts from patients with TAO exhibit increased cell surface IGF-1R display but TSHR levels appear extremely low and similar to those in controls. Fibroblasts were stained with anti-IGF-1R or anti-TSHR Abs as described in “Methods” and subjected to flow cytometry. The grey open histograms (IGF-1R) and dotted histograms (TSHR) represent staining with isotype control Abs. The data represent results from 3 different donors with TAO and 3 without autoimmune disease.

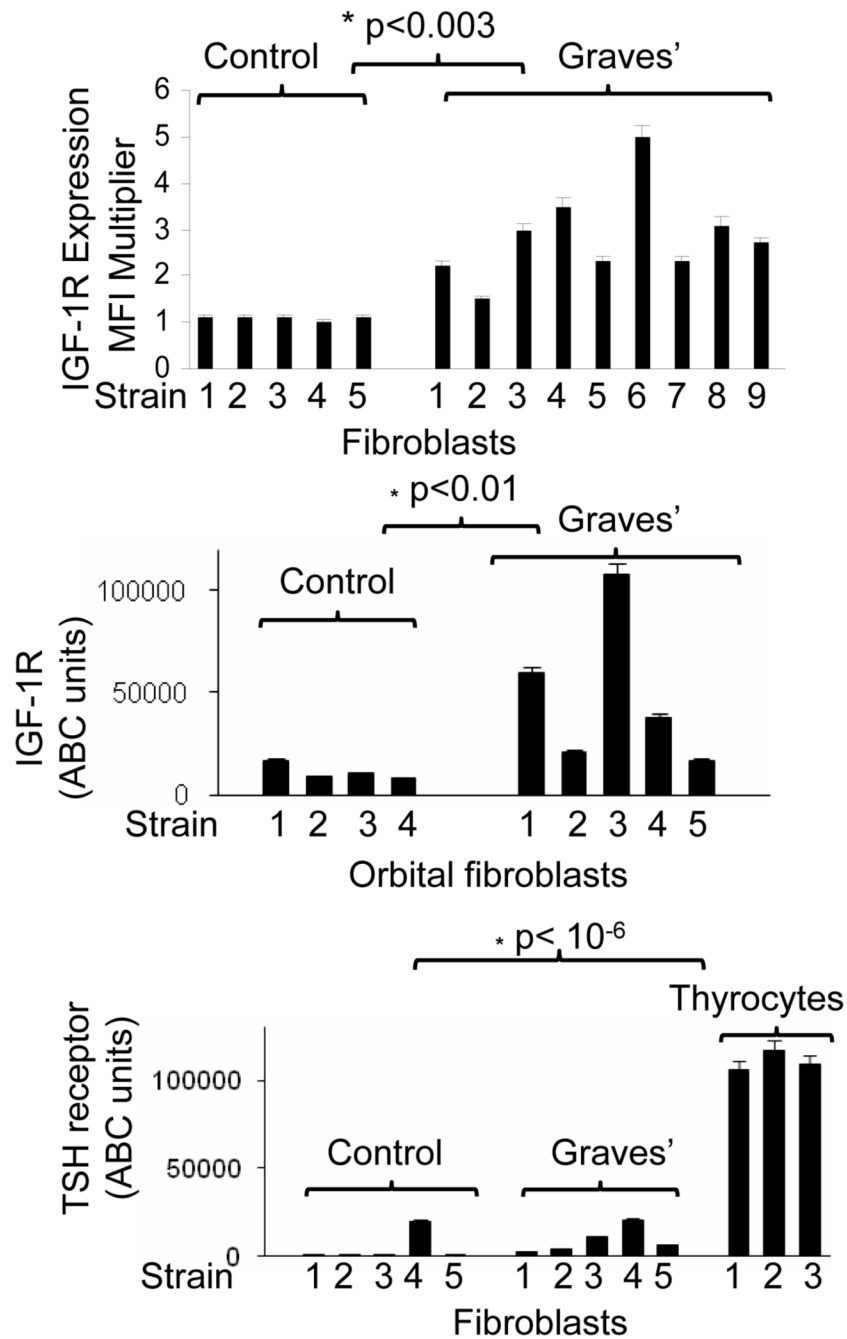


Figure 2.

(A) Multiple strains of orbital fibroblasts from patients with TAO (n=9) express increased IGF-1R expression compared to fibroblasts from control donors (n=5). IGF-1R levels were determined and expressed as a multiple of isotype fluorescence (Mean fluorescent Intensity Multiplier; *p<0.003). (B) IGF-1R molecule density is elevated in multiple strains of orbital fibroblasts from patients with TAO (n=5) compared to control strains (n=4). Quantification of the relative Ab binding to cell surface IGF-1R was determined by ABC analysis, as described in "Methods" section (*p<0.01 TAO vs control). (C) TSHR molecular densities are extremely low and similar in multiple strains of orbital fibroblasts from patients TAO GD (n=5) compared to control strains (n=5). Thyrocyte strains (n=3) display substantially higher levels of TSHR.

Quantification of relative Ab binding to TSHR was determined by ABC analysis, as described in “Methods” section (* $p < 10^{-6}$, fibroblasts vs thyrocytes).

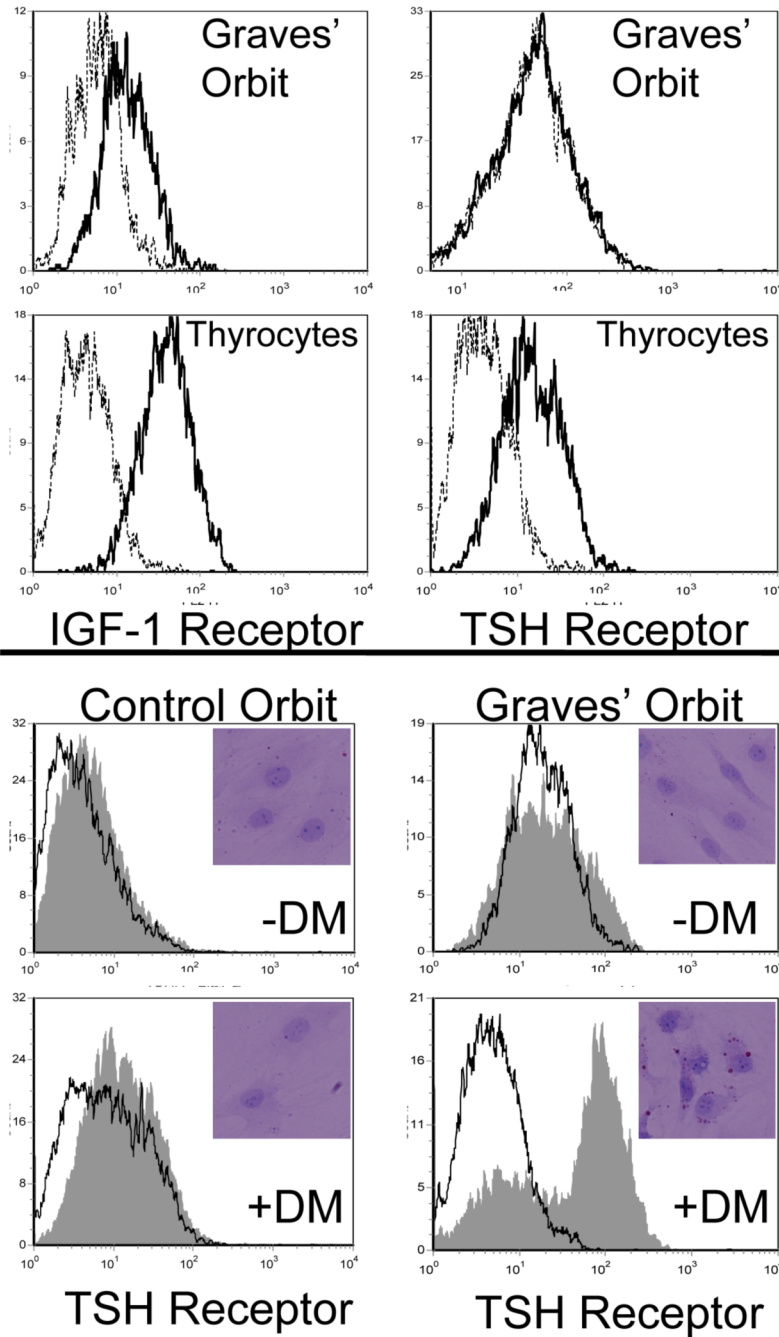


Figure 3.

(A) Paired analysis of IGF-1R (left panels) and TSHR (right panels) in orbital fibroblasts from patients with TAO (top) and thyrocytes (bottom). Orbital fibroblasts and thyrocytes were stained with anti-IGF-1R or anti TSHR Abs as described in “Methods” and subjected to flow cytometry. Dotted histograms represent staining with isotype control Abs. (B) Orbital fibroblasts from control donors and those with TAO were subjected to standard incubation (-DM) or the medium described in “Methods” to promote differentiation into adipocytes (+DM). They were then stained with either anti-TSHR Abs or Oil Red O. The former were subjected to flow cytometry and the latter were examined by light microscopy (insets).

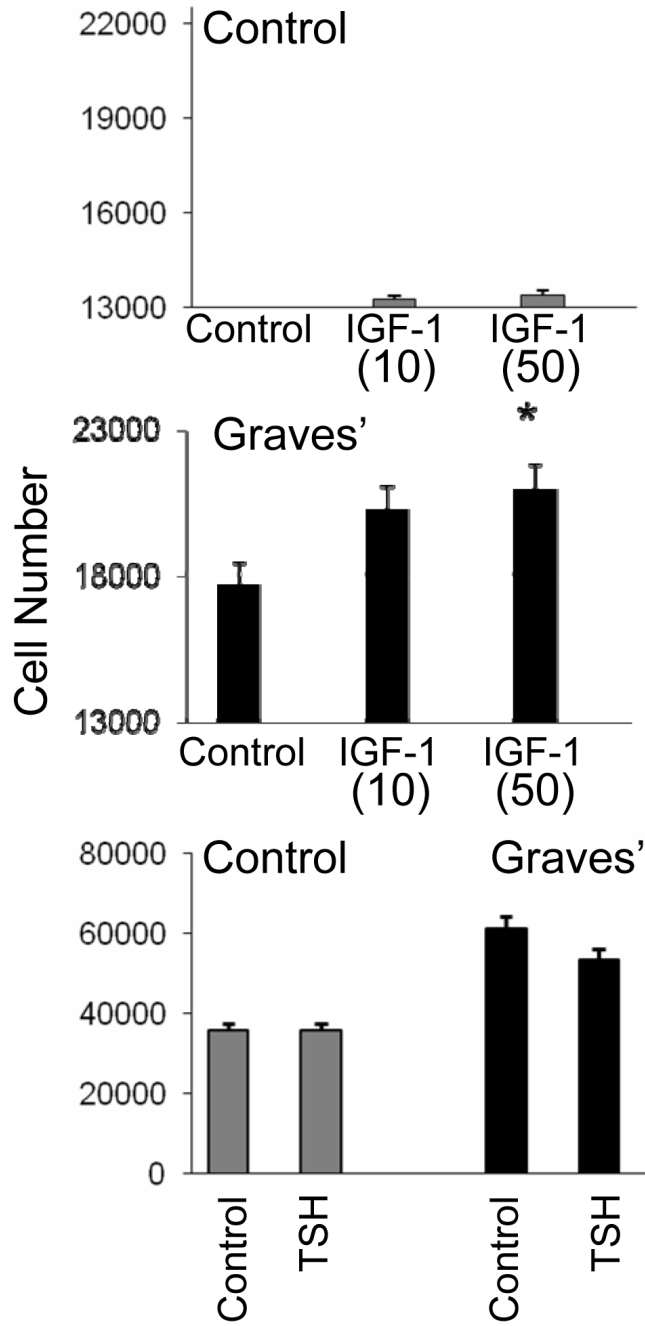


Figure 4. Effects of IGF-1 and rTSH on proliferation of orbital fibroblasts from donors without (control) or with Graves' disease. IGF-1 enhances expansion of orbital fibroblasts from patients with TAO compared to control fibroblasts while TSH does not. Cell number was assessed as described in "Methods" after 7 days in culture with IGF-1 (10 or 50 ng/ml) or TSH (2 mU/ml). Data are expressed as the mean \pm SEM derive from 5 independent experiments (* $p < 0.05$ vs control).

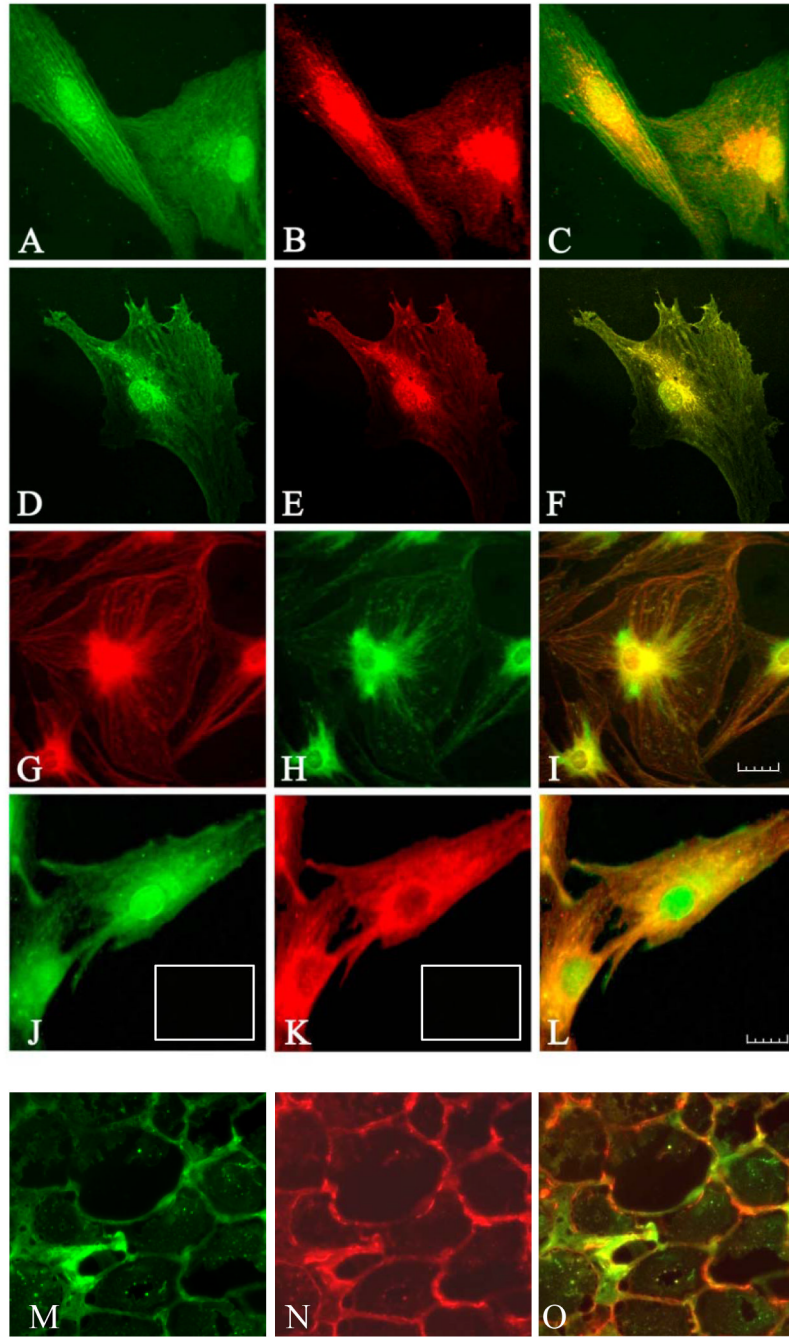


Figure 5. (panels A-F). Immunofluorescence staining for IGF-1R β (red) and TSHR (green) demonstrates co-localization of the two proteins (yellow) by confocal microscopy in orbital fibroblasts from a patient with severe TAO (panels A-C) and thyrocytes (panels D-F). In the merged images, co-localization appears as yellow or orange (panels C and F). Panels G-I, Confocal images using a different pair of Abs show IGF-1R β (green) and TSHR (red), and co-localization of IGF-1R β and TSHR (yellow) in fibroblasts. Note a similar co-localization pattern of these receptors. Panels J-L, Immunofluorescence staining for TSHR (green) and IGF-1R α (red) in orbital fibroblasts demonstrates a different co-localization pattern than that for IGF-1R β . The merged image (panel L) demonstrates co-localization (yellow to orange). Orbital fibroblasts

and thyrocytes were cultured and fixed as described in “Methods” and visualized with a Nikon PCM 2000 confocal microscope. *Scale bar, 25 μ m.* Orbital connective tissue from a patient with TAO also stains for TSHR (panel M, green), IGF-1R (panel N, red), and also demonstrated receptor co-localization when the images are merged (panel O, orange). In sets in Panels J and K, isotype control Abs.

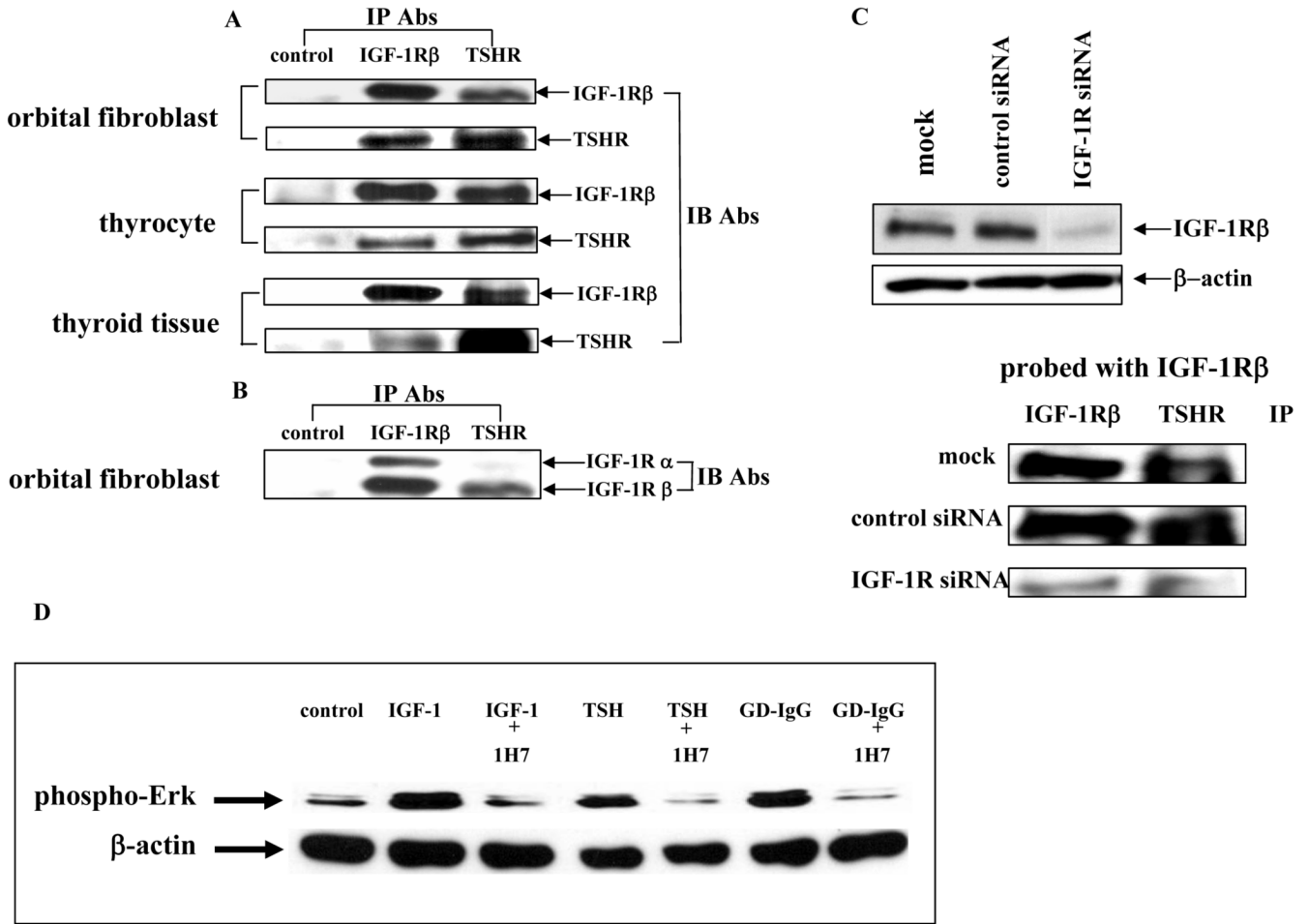


Figure 6. (A and B) Western blot analysis of proteins from orbital fibroblasts, thyrocytes and thyroid tissue subjected to immunoprecipitation with either anti-IGF-1Rβ or anti-TSHR antibodies. Confluent cultures were harvested. Cells and tissue were solubilized and subjected to precipitation (IP) with anti-IGF-1Rβ, anti-TSHR or anti-IL-6 receptor Abs (control) as described in “Methods”. Precipitated proteins were separated with SDS-PAGE, transferred and immunoblotted with (IB) anti-IGF-1Rα, anti-IGF-1Rβ or anti-TSHR Abs. (C) Knocking-down IGF-1R expression with specific siRNA disrupts the TSHR/IGF-1Rβ complex. Cells were prepared as described above after they had been treated with siRNA for IGF-1R. They were then subjected to Western analysis (upper) or IP (lower) and probed as indicated in the figure. (D) Western blot analysis of ERK activation in confluent thyrocytes treated with IGF-1 (10 ng/ml), rhTSH (1 mU/ml) or GD-IgG (100 ng/ml) without or with the blocking anti-IGF-1R mAb, 1H7 (5 μg/ml) for 15 min. Cells were harvested and proteins subjected to western blot analysis for phospho-ERK levels at 42/44 kDa. Loading equivalence was confirmed by blotting with anti-β actin. Signals were generated as described in “Methods”. Relative densities, corrected for their respective β-actin signals were: control, 0.250; IGF-1, 0.775; IGF-1 + 1H7, 0.1962; TSH, 0.432; TSH + 1H7, 0.053; GD-IgG, 0.506; GD-IgG + 1H7, 0.0439